Structural design and theoretical analysis of achieving the net gain of SPASER

Li Wenchao[1], Zhao Lingling[2], Li Zhiquan[2], Zhu Jun[3], Tong Kai[2], Wang Zhibin[2]

(1. School of Control Engineering, Northeastern University at Qinhuangdao, Qinhuangdao 066004, China;
2. College of Electrical Engineering, Yanshan University, Qinhuangdao 066004, China;
3. College of Electronic Engineering, Guangxi Normal University, Guilin 541004, China)

Abstract: An improved metal-insulator-metal(MIM) waveguide structure was used to realize the potential of surface plasmon amplification by stimulated emission of radiation (SPASER) as amplification, although a major problem is that the net gain of SPASER equals zero, which makes it unsuitable for amplification. With the use of a theoretical Hamiltonian model as basis, the lasing conditions were obtained. The numerical calculations of these conditions show that overcoming the inherent feedback and eliminating the surface plasmon (SP) net gain are feasible by using the improved MIM waveguide structure, which can achieve stable SP excitons in less than 100 fs. This study shows that the improved SPASER amplifies with a response time of 100 fs, a bandwidth of 1.5−2.0 THz, and an SP gain of 30−60 dB. SPASER amplifier research provides theoretical and technological foundation for large-scale integrated photonic chips.

Key words: surface plasmon polaritons; metal-insulator-metal waveguide; bistable amplification

CLC number: O23 **Document code:** A **Article ID:** 1007−2276(2015)09−2684−06

表面等离子激元净放大的结构设计与理论分析

李文超[1],赵玲玲[2],李志全[2],朱 君[3],童 凯[2],王志斌[2]

(1. 东北大学秦皇岛分校 控制工程学院, 河北 秦皇岛 066004; 2. 燕山大学 电气工程学院,
河北 秦皇岛 066004; 3. 广西师范大学 电子工程学院,广西 桂林 541004)

摘 要: 连续波发生器的 SPASER(Surface Plasmon Amplification by Stimulated Emission of Radiation)相当于净放大等于零,不能作为放大器使用,文中采用改进的 MIM 波导结构实现 SPASER 作为放大器可能性。利用汉密尔顿函数的理论模型得到了放大器激射条件,数值计算表明:采用改进的 MIM 波导结构实现解决 SPASER 的内反馈问题和消除 SP 的净增益问题是可行的; 改进结构在不到 100 fs的时间里实现了 SP 激子数的稳定水平;改进 SPASER 放大器响应时间为 100 fs,带宽为 1.5~2 THz,SP 的放大增益在 30~60 dB 范围。上述研究成果将为大规模集成光子学芯片设计提供了理论和技术基础。

关键词: 表面等离子激元; 金属−绝缘体−金属波导; 双稳态放大

收稿日期:2015−01−17; **修订日期**:2015−02−23

基金项目:国家自然科学基金(61172044);广西自然科学基金(2015GXNSFBA139257);广西师范大学博士科研启动基金

作者简介:李文超(1981−),男,讲师,博士生,主要从事非线性光电方面的研究。Email:chao121328@sohu.com

通讯作者:朱君(1985−),男,硕士生导师,博士,主要从事微纳器件设计与制作方面的研究。Email:zhujun1985@gxnu.edu.cn

0 Introduction

Surface plasmon (SP) waves are interactions among free charges that can migrate in an electromagnetic field and a conductor. Electromagnetic waves that propagate on the surface of the conductor have an energy quantum called surface plasmon polaritons (SPPs). SPPs that spread along the metal surface have exponentially decaying fields (evanescent fields) that are perpendicular to the surface[1-4]. Therefore, the electromagnetic energy of SPPs is strongly confined to the vicinity of the surface, which significantly enhances the near-field intensity near the metal surface and makes SPP excitation and electromagnetic distribution very sensitive to various features of the surface (e.g., changes in morphology and permittivity)[5-9]. The key question in SPP technological applications is the improvement of propagation lengths while oscillation intensity is reduced to $1/e$[10]. Given strong attenuation caused by ohmic effects, propagation length with a visible light wavelength of 500 nm is approximately 2 μm. Even with long-range SPP waveguide technology, the propagation length is only about 22 μm[11]. Current SPP propagation and related research reports that SPASER is the smallest laser and the first nanoscale active device that operates in the visible wavelength or a wider range[12]. In the past 10 years, SPASER research has made the following significant achievements: the definition of SPs and establishment of a theoretical manipulation model, the determination of the life cycle of quantum structure SPs, research on dimensionless gain characteristics in systems and discussion of scattering conditions, and excitation of plasma oscillator with a high Q value and a fixed two-dimensional array structure. These achievements in the production of localized spatial and temporal coherence of SPASER amplifiers provide excellent conditions[13-21]. However, because of nonlinear gain saturation, the inherent inner feedback of SPASER leads to very low population inversion in continuous wave mode, which indicates that SPASER as a continuous wave generator corresponds to zero net amplification and thus cannot be used as an amplifier. To address these issues, this study uses the improved MIM waveguide structure to overcome the inherent feedback and elimination of the SP net gain[22-26]. Results of a study of the design feasibility and parameters have a certain reference value for the integration of SPASER with a bistable SP wave amplifier.

1 Theoretical foundation of SPASER

1.1 SPASER

To describe the physical processes of the bistable SPASER amplifier, we need to solve the eigenmode equation of the SP wave in waveguide boundary conditions. The SP eigenmodes at the metal surface can be expressed by the wave equation

$$\nabla \Theta(r) \nabla \varphi_n(r) = s_n \nabla^2 \varphi_n(r) \tag{1}$$

where n is the mode number; S_n is the corresponding eigenvalue, and $\Theta(r)$ is the characteristic function. The value of r is 1 in the metal component and 0 in the dielectric. The eigenvalues S_n are real numbers in the range $0 \leqslant S_n \leqslant 1$. The eigenmodes are normalized by integration over the volume $\int_V |\nabla \varphi_n(r)|^2 d^3 r = 1$. ω_n is the physical frequency of the SPs, given by $\mathrm{Re}[s\omega_n] = s_n$, where $s(\omega) = \varepsilon_d / [\varepsilon_d - \varepsilon_m(\omega)]$ refers to Bergman′s spectral parameters. ε_d and ε_m are the dielectric constants for air and metal, respectively.

With the Hamiltonian defined according to Eq.(1), the SPASER Hamiltonian has the following form:

$$H = H_g + \hbar \sum_p \vec{E}(\vec{r}_p) \vec{d}^{(p)} \tag{2}$$

where H_g is the Hamiltonian of the gain medium, p is an index of the gain medium chromophore, $\vec{r}_p$ is the coordinate vector, and $\vec{d}^{(p)}$ is its dipole moment operator.

1.2 SPASER lasing conditions

In the density matrix, the difference in the diagonal element is used to describe the population

inversion number, while the non-diagonal element corresponds to the transition process. In semi-classical approximation, $\hat{a}_n$ is considered as classic a_n, which is represented as $a_n=a_{0n}\exp(-i\omega t)$, a time-dependent parameter, where a_{0n} is a slowly changing amplitude. The quantum number of the coherent SP for a SPASER transmission mode can be determined by $N_p=|a_{0n}|^2$. In the standard method, by exchanging with H, the satisfied equation is obtained and solved to realize the time-dependent variations. According to the above theoretical analysis, the SPASER lasing conditions can be written as:

$$\frac{(g+G_{12})^2}{g_nG_{12}(\omega_{21}-\omega_n)^2+(G_{12}-g_n)^2}\overset{\circ}{a}_p|\omega_{12}^{(p)}|^2n_{21}^{(p)}=1 \tag{3}$$

where ω_{21} is the gain transition frequency, ω_n is the plasma frequency, $n_{21}^{(p)}$ is the population inversion number of the p-th chromophore.

2 Theoretical description of structural design

We present a theoretical description of the structure (Fig.1), which includes the ordinary and the improved MIM waveguide structures.

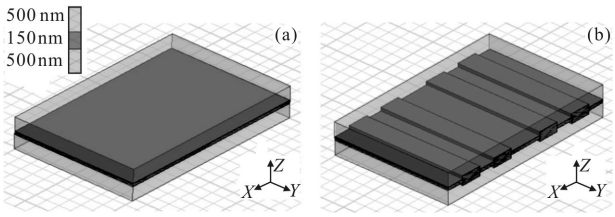

Fig.1 Ordinary MIM waveguide structure (a) and improved MIM waveguide structure (b)

2.1 Physical description of SPASER amplifier

A bistable amplifier composed of a saturable absorber implanted in the SPASER structure is a prominent feature of this project. Generally, bistability is the result of nonlinearity caused by the presence of a saturable absorber in the system. The saturable absorber is a chromophore whose absorption overlaps with SP emission lines yet only indirectly absorbs the radiation produced by the pump SPASER[21-24,27].

Physically, when the ρ_a phase of the coherent SP field is determined by synchronous noise, SPASER activity is the result of spontaneous symmetry breaking. The mathematics indicates non-trivial solutions in the differential equations for the description of SPASER. The stable part of the isolated solution suggests the following conclusions: with an increasing pumping rate, the critical pumping rate g appears, in which process the saturated absorber density ρ_a also increases; when the threshold g reaches a given ρ_a, the nonzero N_n branch interrupts, whereas the branches of $N_n=0$ and $N_n>0$ are stable and can retain their state. The transition between these two stable states can be achieved by increasing or decreasing the number of the SP quantum in the transmission mode, whose relationship is written as $\rho_a=3\rho$. Therefore, SPASER with a saturable absorber can serve as a nano-storage unit and quantum amplifier equipment based on bistability, whose dynamic response is at the femtosecond level.

2.2 Equation for population inversion in structure

The SPASER rapidly relaxes to zero with a small initial particle number N_n, whereas gain medium particles quickly reach a high n_{21}, that is, a decreasing SP mode number transmitted by SPASER eliminates the stimulated radiation. The SPASER remains stable for a long time, although it pumps continuously. By contrast, when the initial number of SP excitons is large enough, the SP population in the SPASER mode reaches $N_n\approx 60$. The SPASER exceeds this state in less than 100 fs because of the relaxation oscillations. As the SP population stabilizes, the population inversion n_{21} of the gain medium is fixed at a low level, which is a typical CW regime of the SPASER. The experiment shows that this state is maintained as long as the pumping supports the population inversion.

Under pulse pumping, the population inversions generated by a short pulse in the bistable SPASER are expressed by Eqs.(4)-(6).

$$\dot{\bar{\rho}}_{12}^{(p)}=-[i(\omega-\omega_{12})+\Gamma_{12}]\bar{\rho}_{12}^{(p)}+in_{21}^{(p)}\Omega_{12}^{(p)*} \tag{4}$$

$$\dot{n}_{12}^{(p)}=-4\mathrm{Im}[\bar{\rho}_{12}^{(p)}\Omega_{21}^{(p)}]-\gamma_2(1+n_{21}^{(p)})+g(1-n_{21}^{(p)}) \quad (5)$$

$$\dot{a}_{\mathrm{on}}=[i(\omega-\omega_n-\gamma_n)]a_{\mathrm{on}}+i\sum_p \rho_{12}^{(p)*}\Omega_{12}^{p} \quad (6)$$

where $\dot{\bar{\rho}}_{12}^{(p)}$ is a non-diagonal element of the density matrix of the $p-$th chromophore; $n_{21}^{(p)}$ is the population inversion number, that is, the difference in the diagonal element of the density matrix; the constant Γ_{12} is a representative of the polarization relaxation; $\Omega_{12}^{(p)}=-Ad_{12}^{(p)}\nabla\varphi_n(\vec{r}_p)a_{0n}/\hbar$ is the Rabi frequency for the spasing transition in the $p-$th chromophore; $d_{12}^{(p)}$ is the corresponding transitional dipole element; and γ_2 is the decay rate.

3 Model validation of finite element analysis

For the structures in Fig.1, which were compared for model validation, we use finite element method to model the numerical computation. Changes in eigenmodes determine the accuracy of the structure of SPP propagation. Based on these results, the model eigenmode for the structures is solved. The results are shown in Fig.2 and Fig.3, which present the electromagnetic field distributions for the two MIM waveguide structures. These distributions suggest that the improved MIM waveguide structures do not change the electromagnetic field distribution, which verifies the accuracy of the model, and that the SP net gain in the model is feasibly corrected.

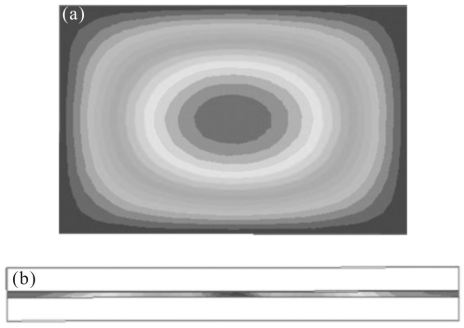

Fig.2 Electromagnetic field distribution of the ordinary electric field (a) and magnetic field (b)

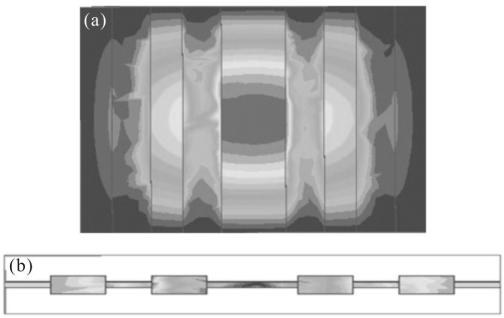

Fig.3 Electromagnetic field distribution of the improvement of electric field (a) and magnetic field (b)

4 Results of simulation of SP excitons

The SP exciton number in the low and high states for the SPASER amplifier′s transience of modification is shown in Fig.4. The SPASER, which has a series of relaxation oscillations when the initial population N_n is less than the threshold, relaxes rapidly when the N_n approaches zero because of the transition of the enhanced energy in the metal to the SP model. In Fig.4(b), when the initial population N_n is large enough, the number exceeds the initial population within a few hundred femtoseconds. Theoretical

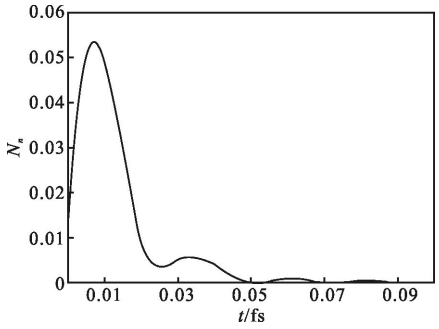

(a) Bistable of low state

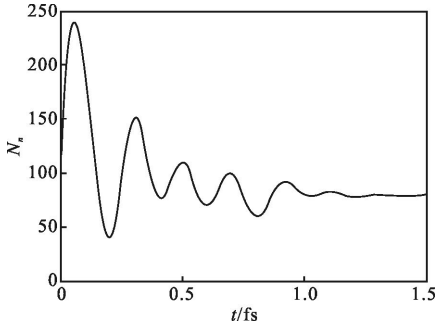

(b) Bistable of high state

Fig.4 Curve of SP excitions number

analysis shows that when the SP exciton number stabilizes, it remains in this state for a long time.

To further characterize the ampli fication of the SPs, the contrast of power spectral density for the SPASER amplifier is illustrated in Fig.5, which shows that the loss in the SPASER amplifier is significantly smaller than that in the general SP lasing structure. Theoretical analysis and simulation results indicate that the performance indices of the developed bistable SPASER amplifier can reach a response time of 100 fs, a bandwidth of 1.5 to 2.0 THz, and an SP amplification gain of 30 to 60 dB.

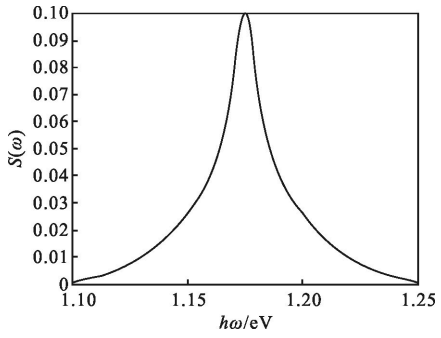

(a) Ordinary SP

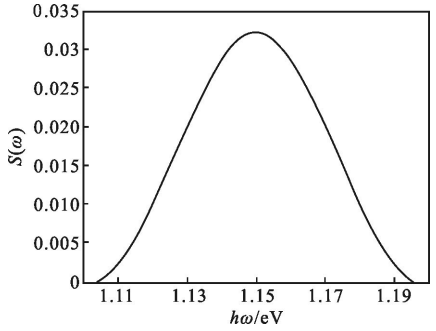

(b) SPASER amplifier

Fig.5 Contrast of $S(\omega)$

5 Conclusion

The optical structures and devices of propagating SPPs provide an effective way for the manipulation of photons at the nano-scale, the accomplishment of the all-optical, and the development of the smaller, more efficient nanophotonics. The most signification result is the study of the improved MIM waveguide structures, analyzing the optical bistability characteristics, simultaneously. Combined with theoretical analysis and simulation results, we can achieve that overcoming the inherent feedback and elimination of the SP net gain are feasible by using the improved MIM waveguide structure, which can achieve a stable level of SP excitons in less than 100 fs time, meanwhile the study obtain the performance indexes of the developed bistable SPASER amplifier. SPASER amplifier research will provide theoretical and technology foundation for large-scale integrated photonic chip.

References:

[1] Andrianov E S, Pukhov A A, Dorofeenko A V, et al. Dipole response of spaser on an external optical wave [J]. ***Optics Letters***, 2011, 36(21): 4302-4034.

[2] Lin J, Mueller J P B, Wang Q, et al. Polarization-controlled tunable directional coupling of surface plasmon polaritons[J]. ***Science***, 2013, 340(6130): 331-340.

[3] Fedyanin D Y. Toward an electrically pumped spaser [J]. ***Optics Letters***, 2012, 37(3): 404-406.

[4] Lu Y J, Kim J. Chen H Y, et al. Plasmon nanolaser using epitaxially grown silver film [J]. ***Science***, 2012, 337(6093): 450-453.

[5] Bergman D J, Stockman M I. Surface plasmon amplification by stimulated emission of radiation quantum generation of coherent surface plasmons in nanosysterms [J]. ***Physical Review Letters***, 2003, 90(2): 027402.

[6] Stockman M I. The spaser as a nanoscale quantum generator and ultrafast amplifier [J]. ***Journal of Optics***, 2010, 12(2): 024004.

[7] Faryad M, Lakhtaki A. Granting-coupled excitation of multiple surface plasmon-polarton waves[J]. ***Physical Review A***, 2011, 84(3): 033852.

[8] Noginov M A, Zhu G, Belgrave A M, et al. Demonstration of a spaser-based nanolaser [J]. ***Nature***, 2009, 460(7259): 1110-1112.

[9] Brongersma M L, Shalaev V M. Applied physics the case for plasmonics[J]. ***Science***, 2010, 328(10): 440-441.

[10] Di Martino G, Sonnefraud Y, Kena-Cohen S, et al. Quantum statistics of surface plasmon polaritons in metallic stripe waveguides[J]. ***Nano Letters***, 2012, 12(5): 2504-2058.

[11] Wang B, Zhang X, Garcia-Vidal F J, et al. Strong coupling of surface plasmon polaritons in monolayer graphene sheet

arrays[J]. ***Physical Review Letters***, 2012, 109(7): 073901.

[12] Stockman M I. Spaser action, loss compensation and stability in plasmonic systems with gain [J]. ***Physical Review Letters***, 2011, 106(15): 156802.

[13] Ge Yuanjing, Zhang Guangqiu, Chen Qiang. Plasma Science Technology and Its Application in Industry [M]. Beijing: China Light Industry Press, 2007

[14] Georges A T, Karatzas N E. Optimizing the excitation of surface plasmon polaritons by difference-frequency generation on a gold surface[J]. ***Physical Review B***, 2012, 85(15): 155442.

[15] Martín-Becerra D, Temnov V V, Thomay T, et al. Spectral dependence of the magnetic modulation of surface plasmon polaritons in noble/ferromagnetic/noble metal films [J]. ***Physical Review B***, 2012, 86(3): 035118.

[16] Lee S Y, Lee I M, Park J, et al. Role of magnetic induction currents in nanoslit excitation of surface plasmon polaritons [J]. ***Physical Review Letters***, 2012, 108(21): 213907.

[17] Hong Xiaogang, Xu Wendong, Zhao Chengqiang. Optimal design of surface plasmon resonance films structure [J]. ***Acta Optica Sinica***, 2010, 30(7): 2164-2169.

[18] Zheludev N I, Prosvirnin S L, Papasimakis N, et al. Lasing spaser[J]. ***Nature Photonics***, 2008, 2(6): 351-354.

[19] Shubina T V, Gippius N A, Shalygin V A, et al. Terahertz radiation due to random grating coupled surface plasmon polaritons[J]. ***Physical Review B***, 2011, 83(16): 165312.

[20] Yin Y, Wu M W. Kinetic theory of surface plasmon polariton in semiconductor nanowires[J]. ***Physical Review B***, 2013, 87(16): 165412.

[21] Polanco J, Fitzgerald R M, Maradudin A A. Scattering of surface plasmon polaritons by one-dimensional surface defects [J]. ***Physical Review B***, 2013, 87(15): 155417.

[22] Lopez-Rios T. Enhanced Raman scattering mediated by long wave vector surface plasmon polaritons [J]. ***Physical Review B***, 2012, 85(12): 125438.

[23] Siahpoush V, Stondergaard T, Jung J. Green′s function approach to investigate the excitation of surface plasmon polaritons in a nanometer-thin metal film [J]. ***Physical Review B***, 2012, 85(7): 075305.

[24] Stondergaard T, Siahpoush V, Jung J. Coupling light into and out from the surface plasmon polaritons of a nanometer-thin metal film with a metal nanostrip [J]. ***Physical Review B***, 2012, 86(8): 085455.

[25] Warmbier R, Manyali G S, Quandt A. Surface plasmon polaritons in lossy uniaxial anisotropic materials[J]. ***Physical Review B***, 2012, 85(8): 085442.

[26] Koponen M A, Hohenester U, Hakala T K, et al. Absence of mutual polariton scattering for strongly coupled surface plasmon polaritons and dye molecules with a large Stokes shift[J]. ***Physical Review B***, 2013, 88(8): 085425.

[27] Ignatyeva D O, Kalish A N, Levkina G Y, et al. Surface plasmon polaritons at gyrotropic interfaces [J]. ***Physical Review A***, 2012, 85(4): 043804.

[28] Baumeier B, Huerkamp F, Leskova T A, et al. Scattering of surface-plasmon polaritons by a localized dielectric surface defect studied using an effective boundary condition [J]. ***Physical Review A***, 2011, 84(1): 013810.